1521-0111/101/1/56–67$35.00
MOLECULAR PHARMACOLOGY

https://doi.org/10.1124/molpharm.121.000349
Mol Pharmacol 101:56–67, January 2022

Steroidal Antagonists of Progesterone- and Prostaglandin E_1-Induced Activation of the Cation Channel of Sperm [S]

Erick J. Carlson, Gunda I. Georg, and Jon E. Hawkinson

Department of Medicinal Chemistry (E.J.C., G.I.G., J.E.H.) and Institute for Therapeutics Discovery and Development (G.I.G., J.E.H.), University of Minnesota, Minneapolis, Minnesota

Received June 22, 2021; accepted October 23, 2021

ABSTRACT

The cation channel of sperm (CatSper) is the principal entry point for calcium in human spermatozoa and its proper function is essential for successful fertilization. As CatSper is potently activated by progesterone, we evaluated a range of steroids to define the structure-activity relationships for channel activation and found that CatSper is activated by a broad range of steroids with diverse structural modifications. By testing steroids that failed to elicit calcium influx as inhibitors of channel activation, we discovered that medroxyprogesterone acetate, levonorgestrel, and aldosterone inhibited calcium influx produced by progesterone, prostaglandin E_1, and the fungal natural product *l*-sirenin, but these steroidal inhibitors failed to prevent calcium influx in response to elevated K^+ and pH. In contrast to these steroid antagonists, we demonstrated for the first time that the T-type calcium channel blocker ML218 acts similarly to mibefradil, blocking CatSper channels activated by both ligands and alkalinization/depolarization. These T-type calcium channel blockers produced an insurmountable blockade of CatSper, whereas the three steroids produced antagonism that was surmountable by increasing concentrations of each activator, indicating that the steroids selectively antagonize ligand-induced activation of CatSper rather than blocking channel function. Both the channel blockers and the steroid antagonists markedly reduced hyperactivated motility of human sperm assessed by computer-aided sperm analysis, consistent with inhibition of CatSper activation. Unlike the channel blockers mibefradil and ML218, which reduced total and progressive motility, medroxyprogesterone acetate, levonorgestrel, and aldosterone had little effect on these motility parameters, indicating that these steroids are selective inhibitors of hyperactivated sperm motility.

SIGNIFICANCE STATEMENT

The steroids medroxyprogesterone acetate, levonorgestrel, and aldosterone selectively antagonize progesterone- and prostaglandin E_1-induced calcium influx through the CatSper cation channel in human sperm. In contrast to T-type calcium channel blockers that prevent all modes of CatSper activation, these steroid CatSper antagonists preferentially reduce hyperactivated sperm motility, which is required for fertilization. The discovery of competitive antagonists of ligand-induced CatSper activation provides starting points for future discovery of male contraceptive agents acting by this unique mechanism.

Introduction

A major focus of research on the cation channel of sperm (CatSper) has been to understand its impact on fertilization (Quill et al., 2001; Ren et al., 2001). Activation of CatSper triggers calcium influx and release from internal stores leading to oscillations in intracellular calcium ($[Ca^{2+}]_i$) that originate in the flagellum and spread to the neck and head (Torrezan-Nitao et al., 2021). Calcium entry drives hyperactivated motility (HAM) that is required for fertilization (Quill et al., 2003; Qi et al., 2007). The recent cryo-electron microscopy structure of CatSper (Lin et al., 2021) shows that the pore-forming subunits CatSper1–4 (Ren et al., 2001; Quill et al., 2003; Qi et al., 2007) are stabilized by a pavilion-like structure consisting of the auxiliary subunits β (Liu et al., 2007), γ (Wang et al., 2009), δ (Chung et al., 2011), and ε (Chung et al., 2017) via their large extracellular domains. The ζ subunit (Chung et al., 2017) and EF-Hand Calcium Binding Domain 9 (Hwang et al., 2019) associate with the cytoplasmic face of the channel. Additional closely interacting transmembrane proteins are CatSperη, THEM249, and SLCO6C1 (Lin et al., 2021). The expression and association of all CatSper subunits is required for channel function and fertilization. Male mice deficient in CatSper1, 2, 3, 4, and δ are infertile and display no other observable

This work was supported by National Institutes of Health National Institute of Child Health and Human Development and the University of Minnesota Vince and McKnight Endowed Chairs.
This work was previously presented in thesis "The Development of Potential Male Contraceptives Via Inhibition of CatSper and also GBA2" and a talk given by E.J.C. as part of the MIKIW meeting at the University of Kansas on April 14, 2019.
No author has an actual or perceived conflict of interest with the contents of this article.
dx.doi.org/10.1124/molpharm.121.000349.

[S] This article has supplemental material available at molpharm.aspetjournals.org.

ABBREVIATIONS: ABHD2, α/β hydrolase domain-containing protein 2; 2AG, 2-arachidonoylglycerol; ALDO, aldosterone; $[Ca^{2+}]_i$, intracellular calcium; BSA, bovine serum albumin; CASA, computer-assisted sperm analysis; CatSper, cation channel of sperm; CCB, calcium channel blocker; DMA, dimethylandrolone; HAM, hyperactivated motility; LNG, levonorgestrel; MBF, mibefradil; MPA, medroxyprogesterone acetate; PGE_1, prostaglandin E_1; PROG, progesterone; SAR, structure-activity relationships; THDOC, tetrahydrodeoxycorticosterone.

phenotype (Ren et al., 2001; Quill et al., 2003; Qi et al., 2007; Wang et al., 2009). The auxiliary subunits CatSperζ and EF-Hand Calcium Binding Domain 9 form a complex that regulates channel function by acting as a pH and Ca^{2+} sensor, and mice deficient in either or both subunits were severely subfertile, and their sperm could not achieve HAM (Chung et al., 2017; Hwang et al., 2019). Given its obligatory role in fertilization, it is not surprising that mutations in genes coding for pore-forming and auxiliary CatSper subunits have been identified as the causative effects of male infertility in several families (Avidan et al., 2003; Avenarius et al., 2009; Hildebrand et al., 2010; Shu et al., 2015; Brown et al., 2018; Luo et al., 2019).

The endogenous compounds progesterone (**1**, PROG) and prostaglandin E_1 (**2**, PGE_1) (Fig. 1) elicit a large calcium influx into mature sperm (Blackmore et al., 1990; Schaefer et al., 1998; Shimizu et al., 1998) that has been shown to be mediated by CatSper (Lishko et al., 2011; Strunker et al., 2011). Membrane depolarization and intracellular alkalization, cyclic nucleotides (cAMP, cGMP), zona pellucida glycoproteins, and bovine serum albumin (BSA) activate the channel (Sun et al., 2017). In addition, certain endocrine disrupting chemicals (Schiffer et al., 2014; Rehfeld et al., 2020), odorants (Brenker et al., 2012), and the flavorant anethole (Luo et al., 2020) caused a rapid influx of calcium into sperm via CatSper activation, whereas certain environmental toxicants inhibited PROG-induced CatSper activation (Yuan et al., 2020; Zhang et al., 2020). With the identification of the first subunit CatSper1 in 2001, CatSper represented an excellent target for male contraception (Ren et al., 2001). Indeed, in certain infertility cases, sperm from otherwise healthy men failed to respond to a PROG stimulus (Smith et al., 2013). This observation validated the hypothesis that compounds able to prevent PROG-induced influx of Ca^{2+} by CatSper could serve as contraceptives, which is strengthened by the finding that the CatSper inhibitor HC-056456 greatly reduced both in vitro and in vivo fertilization in mice (Curci et al., 2021).

To understand the structure-activity relationships (SARs) for steroid activation of CatSper, we determined the ability of PROG analogs, progestins including female contraceptive agents, and other steroids to increase $[Ca^{2+}]_i$ in human sperm using a fluorescent calcium assay (Syeda et al., 2016). A broad range of modifications of the PROG scaffold are tolerated. As structural modifications to a ligand can lead to substantial changes in its pharmacological activity (Dosa and Amin, 2016), steroids that were weak or inactive as activators were tested for their ability to block CatSper activation by PROG, PGE_1, and the natural product *l*-sirenin (**3**, Fig. 1). Surprisingly, the clinically used progestins medroxyprogesterone acetate (**4**, MPA, Fig. 2) and levonorgestrel (**5**, LNG) as well as the mineralocorticoid aldosterone (**6**, ALDO) inhibited the activation of CatSper by PROG, PGE_1, and *l*-sirenin.

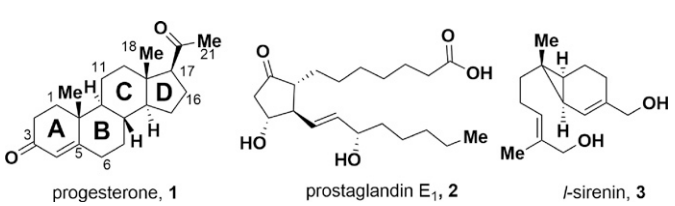

Fig. 1. Structures of CatSper activators PROG, PGE_1, and *l*-sirenin.

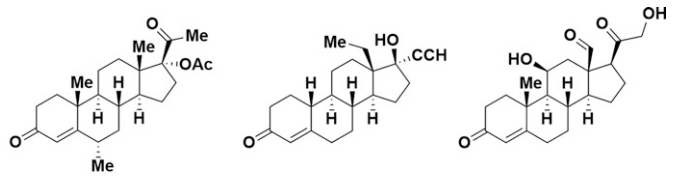

Fig. 2. Structures of CatSper antagonists MPA, LNG, and ALDO.

These steroidal antagonists competitively inhibit PROG-induced activation and selectively reduce HAM. In contrast, T-type calcium channel blockers (CCBs) inhibit depolarization/alkalization-induced activation, noncompetitively block PROG-induced activation, and reduce all modes of sperm motility.

Materials and Methods

Chemical Synthesis and Characterization. A detailed description of the sources of chemicals, reaction conditions, and characterization of synthesized compounds can be found in the supplementary information as well as experimental procedures for the synthesis of steroids 2,2-dimethylprogesterone (**18**, Supplemental Scheme 1), 6α-methylprogesterone (**20**, Supplemental Scheme 2) and its respective intermediates, and the two diastereomers of 5,6-epoxyprogesterone (**16** and **17**, Supplemental Scheme 3).

Human Sperm Calcium Influx Assay. Semen from healthy human donors (approved Institutional Review Board protocol 1102M96152) was collected and incubated in a shaker at 37 °C until complete liquefaction was observed (≤1 hour post collection). Sperm samples were analyzed to establish sperm motility and cell density using a hemocytometer. The sample was diluted to 50 mL in low pH/low K^+ buffer containing (in mM): 101 NaCl, 4.69 KCl, 0.2 $MgSO_4$, 0.36 KH_2PO_4, 25 $NaHCO_3$, 0.32 sodium pyruvate, 2.78 glucose, 94 sodium lactate, 0.2 $CaCl_2$, pH 6.7 adjusted with 1N HCl. The sample was washed twice by centrifugation at 800 x *g* for 10 minutes at 10 °C and the final pellet was resuspended in 10 mL low pH/low K^+ buffer containing 10 μM Fluo-4-AM (Life Technologies, Grand Island, NY) with 1 mM probenecid and incubated for 30 minutes at room temperature in the dark. The dye-loaded sperm were diluted to 50 mL with low pH/low K^+ buffer, centrifuged at 800 *x g*, and the pellet was resuspended in 10 mL low pH/low K^+ buffer. Dye-loaded sperm (10 μL) were plated into black clear-bottom 384-well assay plates (Corning 3683) using a Multidrop Combi dispenser and transferred to the FLIPR Tetra (Molecular Devices, Sunnyvale, CA). Inhibitor and opener compounds were added using a Labcyte Echo 550 acoustic dispenser to an inhibitor plate and an opener plate, respectively, and dissolved in low pH/low K^+ buffer. After a 10-second initial fluorescence read, inhibitors (20 μL, 2.5x final concentration) were added from the inhibitor plate to the cell plate, the fluorescence was zeroed, and 2 minutes later openers (10 μL, 4X final concentration) were added from the opener plate, both additions using the FLIPR 384-pipette head (final volume 40 μL). Fluorescence was monitored at 470–495 nm (excitation) and 515–575 nm (emission) for a total of 7 minutes at 2-second intervals. EC_{50} and IC_{50} values were determined from 8-point, 3-fold serial dilutions of openers and inhibitors, respectively, in duplicate. For opener only experiments, a plate containing low pH/low K^+ buffer replaced the inhibitor plate. For inhibition of depolarization/alkalinization-induced activation, a plate containing high K^+/high pH buffer containing (in mM): 10 NaCl, 140 KCl, 0.198 $MgSO_4$, 0.36 KH_2PO_4, 24.99 $NaHCO_3$, 0.32 sodium pyruvate, 2.78 glucose, 94.08 sodium lactate, 2.04 $CaCl_2$ (final 0.65 mM), pH 8.2 adjusted with 1N NaOH replaced the opener plate. Opener dose-response experiments indicated that 3 μM PROG produced a

maximal calcium signal and was used as the high control in all experiments.

Computer-Assisted Sperm Analysis (CASA). Semen collected from healthy male donors (IRB: 1102M96152) was allowed to liquefy at 37 °C for at least 40 minutes. For each mL of semen sample, a conical tube containing 5 mL of HAMs-F10 (Millipore Sigma, St. Louis, MO) was warmed to 37 °C at a 45° angle. After liquefaction, 1 mL of sample was layered beneath the buffer in each tube, which was then incubated at 37 °C in 5% CO_2 for 1 hour. The top 2 mL of the buffer-containing sperm was then carefully removed, combined, and the density was determined using a hemocytometer. If a concentration of $10x10^6$ cell/mL was not achieved, the sample was centrifuged at 400 x *g* for 7 minutes and the pelleted cells were diluted in HAMs-F10 to achieve $10x10^6$ cells/mL. For capacitation, cells (post swim-up) were suspended in HAM's-F10 containing 5% (w/v) BSA and 15 mM $NaHCO_3$ and incubated for 3.5 hours at 37 °C in 5% CO_2 in the presence of test compound or DMSO vehicle. Sperm motility was determined at 37 °C using a CASA system (HTM-IVOS sperm analysis system, version 12.3, Hamilton Thorne Biosciences, Beverly, MA) that measured average path velocity (VAP, μm/s), straight-line velocity (VSL, μm/s), and curvilinear velocity (VCL, μm/s) using ≥10 fields of view containing ≥200 cells.

Data Analysis. Calcium influx EC_{50} and IC_{50} values were calculated using the maximal peak height with the four parameter nonlinear regression equation. Mean ±SD values from ≥3 independent experiments are expressed as pEC_{50} and pIC_{50}, the negative logarithm of the EC_{50} and IC_{50} values. Antagonist dissociation constants (K_B values) were determined by Schild regression analysis (Arunlakshana and Schild, 1959) using activator EC_{50} values in the presence of increasing competitive antagonist using the equation:

$$log(DR-1)=blog[B]-pKB$$

where [B] is the antagonist concentration, b is the slope of the regression, and pK_B is the negative log of the equilibrium dissociation constant. K_B values were also determined from antagonist IC_{50} values using the Leff-Dougall (Leff and Dougall, 1993) form of the Cheng-Prusoff equation:

$$K_B = \frac{IC_{50}}{[2+\left(\frac{[agonist]_f}{EC_{50}}\right)^b]^{\frac{1}{b}}-1}$$

where IC_{50} is the half-maximal blocker concentration, $[agonist]_f$ is the fixed concentration of agonist used for the IC_{50} determination, EC_{50} is the half-maximal opener concentration, and b is the slope factor of the agonist dose-response curve. The CASA velocity measurements were used to calculate linearity of progression [LIN = (VSL/VCL) × 100] and straightness [STR = (VSL/VAP) × 100], which were used to calculate percent total, progressive, and hyperactivated motility. Data were normalized to vehicle-matched controls, represent the percent of the entire population displaying each type of motility and are graphed as the mean ±SEM of ≥3 independent experiments. Statistical significance was determined using a one-way ANOVA corrected for multiple comparisons followed by Dunnett's test to identify significant differences from control indicated by $*P < 0.05$, $**P < 0.005$, $***P < 0.0005$ and $****P < 0.0001$. Data were analyzed with Prism 7.0.5 (GraphPad, San Diego, CA).

Results

ML218 is a CatSper Channel Blocker. CatSper currents are not sensitive to L-type CCBs (Kirichok et al., 2006), but T-type CCBs including mibefradil (**7**) and NNC55-0396 (**8**) (Fig. 3) block CatSper currents (Lishko et al., 2011; Strunker et al., 2011). Using a fluorescent calcium influx assay in human sperm (Syeda et al., 2016), mibefradil inhibited PROG-, PGE_1-, *l*-sirenin-, and high K^+/high pH-induced increase in $[Ca^{2+}]$. In good agreement with previous studies, mibefradil pIC_{50} values ranged from 5.17 to 4.76 corresponding to IC_{50} values of 6.8 to 18 μM (Table 1, Fig. 4, and Supplemental Fig. 1), and 30 μM mibefradil completely blocked influx for all modes of channel opening. In contrast to a previous report (Strunker et al., 2011), we did not observe a mibefradil-induced calcium influx at higher concentrations. The T-type CCB ML218 (Xiang et al., 2011) (**9**, Fig. 3) inhibited PROG-, PGE_1-, *l*-sirenin-, and high K^+/high pH-induced calcium influx with pIC_{50} values ranging from 5.02 to 4.85 corresponding to IC_{50} values of 9.6 to 14 μM (Table 1, Fig. 4, and Supplemental Fig. 2). Similar to mibefradil, ML218 (30 μM) completely blocked influx by all modes of channel activation and did not elicit an influx up to 100 μM (Supplemental Fig. 3).

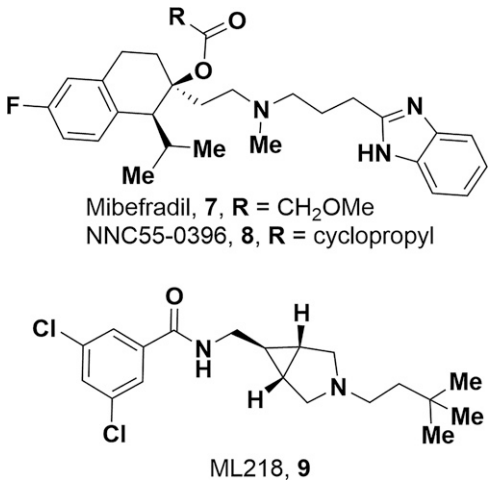

Fig. 3. Structures of T-type calcium channel blockers mibefradil, NNC55-0396, and ML218.

The CatSper Channel Is Activated by a Broad Range of Steroids with Diverse Structural Modifications. PROG potently increased $[Ca^{2+}]_i$ in human sperm cells (pEC_{50} 8.43, EC_{50} 3.7 nM, Table 2, Fig. 5), similar to patch-clamp electrophysiology (EC_{50} 7.7 nM) (Lishko et al.,

TABLE 1
Potencies of mibefradil and ML218 to inhibit calcium influx produced by PROG, PGE_1, *l*-sirenin, and high K^+/high pH in human sperm

Opener	Blocker	pIC_{50}	*n*
PROG	mibefradil	5.17 ± 0.24	7
	ML218	5.02 ± 0.08	4
PGE_1	mibefradil	5.08 ± 0.31	8
	ML218	4.87 ± 0.15	3
l-sirenin	mibefradil	5.09 ± 0.34	5
	ML218	4.85 ± 0.17	3
high K^+/high pH	mibefradil	4.76 ± 0.09	8
	ML218	4.99 ± 0.16	7

Inhibitors were evaluated in the presence of an EC_{80} concentration of each activator (30 nM PROG, 10 nM PGE_1, 3 μM *l*-sirenin). Buffer containing 140 mM K^+, pH 8.2 was added to elicit alkalinization/depolarization calcium influx. pIC_{50} values are expressed as the mean ±SD with the number of independent experiments indicated by *n*.

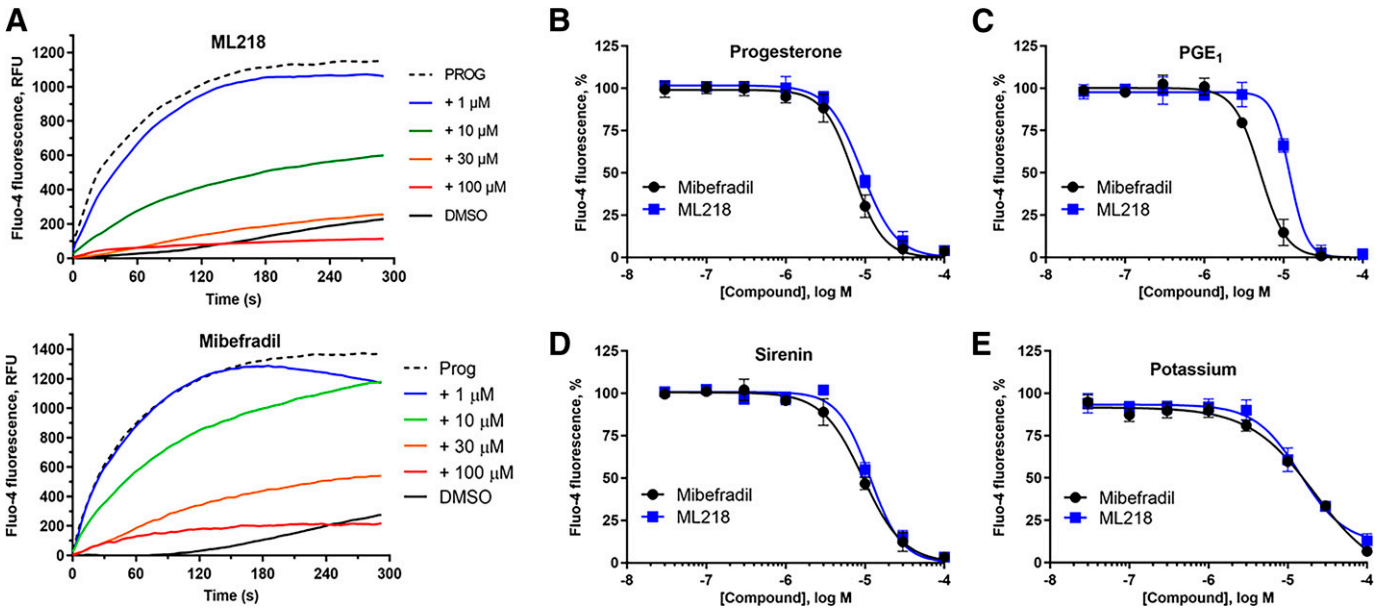

Fig. 4. The T-type CCBs mibefradil and ML218 inhibit PROG-, PGE_1-, *l*-sirenin-, and potassium-induced calcium influx in human sperm. (A) Representative FLIPR traces showing concentration-dependent reduction of PROG-mediated increase in $[Ca^{2+}]_i$ by mibefradil (upper) and ML218 (lower). (B–E) Potencies of mibefradil and ML218 for inhibiting (B) PROG-, (C) PGE_1-, (D) *l*-sirenin-, or (E) high K^+/high pH-induced calcium influx. Ligand-induced activation used EC_{80} concentrations of activator (30 nM PROG, 10 nM PGE_1, 3 μM *l*-sirenin). Buffer containing 140 mM K^+, pH 8.2 was added to elicit alkalinization/depolarization calcium influx (E). The data in B–E are plotted as the mean ±SEM and expressed as a percent of the response produced by each activator alone. IC_{50} and *n* values are in Table 1.

2011) and 10-fold more potent than rapid-mixing calcium fluorimetry (EC_{50} 42 nM) (Strunker et al., 2011). The PROG-induced calcium signal peaked at ~100 seconds and then decayed slowly for up to 300 seconds (Fig. 5A). Others have observed a biphasic response consisting of a maximal transient peak signal at ~50–100 seconds followed by a rapid decay to a minimum at ~150–250 seconds, followed by a lower level signal that was sustained for up to 800 seconds (Strunker et al., 2011; Brenker et al., 2018b). The sustained component of the biphasic response is likely due to opening of store-operated channels, which promote calcium influx (Morris et al., 2015). The longer-lived calcium response in our studies likely precluded observation of the low-level, sustained signal and was likely due to the following factors: (1)

TABLE 2
Potencies for PGE1, *l*-sirenin, PROG, and PROG analogs to elicit calcium influx in human sperm

	#	Steroid	Steroid Alone			+ 30 μM Mibefradil		
			pEC_{50}	E_{max}, %	*n*	pEC_{50}	E_{max}, %	*n*
Activator	**1**	PROG	8.43 ± 0.21	111	7	8.22 ± 0.15	42	3
	2	PGE_1	8.40 ± 0.24	101	8	8.33 ± 0.43	22	5
	3	*l*-sirenin	6.02 ± 0.26	102	3	5.48 ± 0.23	22	3
A Ring or A–B Ring Fusion	**10**	3α,5α-pregnanolone	6.56 ± 0.21	85	5	6.40 ± 0.19	29	3
	11	3α,5β-pregnanolone	6.26 ± 0.25	102	3	6.47 ± 0.22	33	3
	12	3β,5α-pregnanolone	7.16 ± 0.11	99	4	7.08 ± 0.31	38	4
	13	3β,5β-pregnanolone	6.89 ± 0.20	92	4	7.05 ± 0.23	37	4
	14	5α-dihydroprogesterone	6.99 ± 0.05	87	3	6.95 ± 0.12	34	3
	15	5β-dihydroprogesterone	6.87 ± 0.17	95	3	6.67 ± 0.35	20	3
	16	5α,6α-epoxypregnan-3,20-dione[a]	6.08 ± 0.37	83	3	5.96 ± 0.19	12	3
	17	5β,6β-epoxypregnan-3,20-dione[a]	6.38 ± 0.07	84	3	—	<10	3
	18	2,2-dimethylprogesterone[a]	6.31 ± 0.16	99	3	—	<10	3
B Ring	**19**	6β-methylprogesterone[a]	6.58 ± 0.12	90	3	—	<10	3
	20	6α-methylprogesterone[a]	6.16 ± 0.14	96	3	6.62 ± 0.20	18	3
	21	6β-hydroxyprogesterone	6.91 ± 0.10	116	3	6.72 ± 0.09	35	3
	22	5α-hydroxy-6β-methylpregnan-3,20-dione[a]	5.30 ± 0.55	95	3	—	<10	3
C Ring	**23**	11β-hydroxyprogesterone	7.73 ± 0.13	90	5	7.54 ± 0.55	52	4
	24	11α-hydroxyprogesterone	6.90 ± 0.08	100	3	6.93 ± 0.45	32	4
D Ring	**25**	17α-hydroxyprogesterone	7.98 ± 0.35	115	5	8.02 ± 0.36	67	3
	26	3α,5β-THDOC	5.80 ± 0.26	100	3	5.98 ± 0.39	18	4
	27	3α,5α-THDOC	6.05 ± 0.21	96	6	6.20 ± 0.26	37	4
	28	16α-hydroxyprogesterone	6.77 ± 0.18	106	3	6.71 ± 0.27	47	3
	29	17α-acetoxyprogesterone	<5	31	8	<5	37	3
	30	17α-hydroxy-6α-methylprogesterone	6.33 ± 0.10	96	3	—	<10	3

The potency (EC_{50} values, mean ±SD) and maximum response (E_{max}) produced by each compound was determined in the absence and presence of 30 μM mibefradil. E_{max} is expressed as a percent of the response produced by a saturating concentration of PROG (3 μM). The number of independent experiments indicated by *n*. Fitted parameters were not calculated for compounds producing E_{max} < 10%.
[a]Synthesized compound (see Supplemental Schemes 1–3 and Synthetic Procedures for synthesis and characterization).

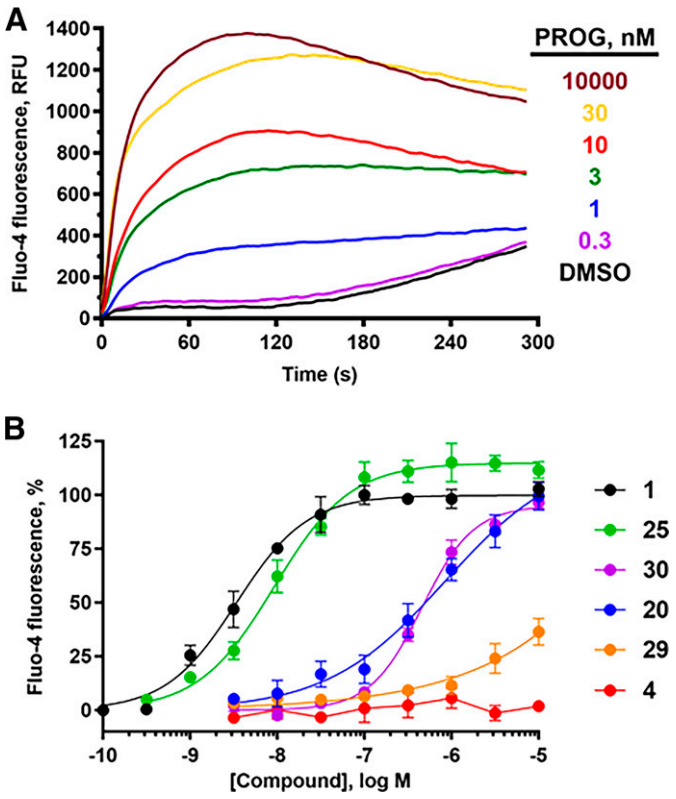

Fig. 5. PROG analogs have a broad range of potencies for eliciting calcium influx in human sperm. (A) Representative FLIPR traces showing the concentration-dependent increase in calcium influx produced by PROG. (B) Concentration-response curves comparing potencies of parent compound PROG and C17- and/or C6-modified analogs: **1**, PROG; **4**, MPA; **20**, 6α-methylprogesterone; **25**, 17α-hydroxyprogesterone; **29**, 17α-acetoxyprogesterone; **30**, 17α-hydroxy-6α-methylprogesterone. Data are plotted as mean ±SEM and expressed as a percent of the response produced by a saturating concentration of PROG (3 μM). EC_{50}, E_{max}, and *n* values are in Tables 2 and 3.

the use of probenecid to block dye efflux, (2) the use of centrifugation to prepare sperm instead of the "swim-up" method, (3) low pH/low K^+ buffer containing 0.2 mM Ca^{2+} instead of human tubal fluid, and (4) the use of Pluronic F-127 to increase dye uptake by others (Strunker et al., 2011). PGE_1 had equivalent potency to PROG, whereas *l*-sirenin was much less potent as previously reported (Syeda et al., 2016).

A broad range of steroids encompassing modifications of each of the steroid rings (structures shown in Supplemental Fig. 4) were evaluated for their ability to elicit calcium influx in sperm. All compounds tested as activators were retested in the presence of the CatSper blocker mibefradil (30 μM, Tables 2 and 3) to confirm that the observed calcium influx was CatSper-dependent. Reduction of both the C3 keto group and C4 unsaturation provided compounds **10–13** that elicited a full response in the influx assay, although were 19- to 150-fold less potent than PROG. Reduction of the A ring decreased potency ~30-fold, although there was little preference for the configuration of the A–B ring fusion since 5α- and 5β-dihydroprogesterone (**14** and **15**) had similar potency. All tested compounds containing either reduced C4 or substituted C5 positions showed little preference for a cis versus trans relationship of the A–B ring fusion (**10–17**). To assess the effect of substitutions on the northern half of the A ring, 2,2-dimethylprogesterone (**18**) was prepared (Supplemental Scheme 1), which showed full efficacy but was 135-fold less potent than PROG. B-ring modifications including hydroxylation or methylation of the 6 position (**19–21**) reduced potency 32- to 190-fold, whereas substitution of both the 5 and 6 positions (**22**) provided a very weak activator likely due to the cumulative effects of both modifications. 11β- and 11α-hydroxylation of the C ring (**23** and **24**) reduced potency 5- and 35-fold, respectively.

D-ring modifications dramatically reduced activity, except for 17α-hydroxylation of PROG (**25**), which was only threefold less potent than the parent steroid (Fig. 5, Table 1). In contrast, hydroxylation of the 21 position to give the tetrahydrodeoxycorticosterones (THDOCs, **26** and **27**) reduced activity a further threefold lower than their corresponding pregnanolones (**10–11**) and were ≥240-fold less potent than PROG. 16α-hydroxylation (**28**) reduced activity 46-fold. Acetylation of the very active 17α-hydroxyprogesterone to give **29** almost ablated activity (Fig. 5). The most profound reduction in activity for the PROG derivatives was observed with the clinically used progestin MPA (**4**) (Table 3) containing the 17α-acetoxy group, which had little effect on $[Ca^{2+}]_i$ up to 10 μM

TABLE 3
Potencies for clinically used progestins, antiprogestins, endogenous steroid hormones and androgens to elicit calcium influx in human sperm

	#	Steroid	Steroid Alone			+30 μM Mibefradil		
			pEC_{50}	E_{max}, %	*n*	pEC_{50}	E_{max}, %	*n*
Progestins and Anti-progestins	**4**	MPA	<5	17	3	—	<10	3
	5	LNG	<5	15	6	—	<10	2
	31	drospirenone	6.28 ± 0.22	115	5	—	<10	4
	32	ulipristal	5.45 ± 0.22	106	3	<5	12	5
	33	mifepristone (RU-486)	5.33 ± 0.30	109	4	—	<10	5
	34	ulipristal acetate	<5	27	3	—	<10	3
	35	segesterone acetate	<5	57	4	—	<10	4
Endogenous	**6**	ALDO	—	<10	3	—	<10	1
	36	testosterone	6.66 ± 0.22	114	3	<5	17	4
	37	17β-estradiol	6.53 ± 0.25	94	3	<5	37	1
Androgens	**38**	11β-methyl-19-nortestosterone	6.37 ± 0.32	85	6	6.27 ± 0.25	15	3
	39	7α-methyl-19-nortestosterone	6.25 ± 0.37	86	7	6.29	26	2
	40	7α,11β-dimethylandrolone	6.06 ± 0.49	80	9	<5	11	3
	41	7β,11β-dimethylandrolone	5.41 ± 0.24	42	5	<5	26	3

The potency (EC_{50} values, mean ±SD) and maximum response (E_{max}) produced by each compound was determined in the absence and presence of 30 μM mibefradil. E_{max} is expressed as a percent of the response produced by a saturating concentration of PROG (3 μM). The number of independent experiments indicated by *n*. Fitted parameters were not calculated for compounds producing E_{max} < 10%.

(Fig. 5). Given the inactivity of 17α-acetoxyprogesterone and MPA, 6α-methylprogesterone (**20**) was synthesized (Supplemental Material 2) to ascertain the effect of B-ring modifications lacking any accompanying C17 modifications. 6α-methylation caused a 190-fold reduction in activity with respect to PROG (Fig. 5) but did not abolish activity as did the 17α-acetoxy modification. This is consistent with the addition of a 6α-methyl group to the potent 17α-hydroxprogesterone (**30**), which reduced its activity 47-fold (Fig. 5). Converting the C3 and C20 ketones to their corresponding ethylene ketals showed a dramatic loss in potency (Supplemental Fig. 5).

Clinically Relevant Steroids Elicit Calcium Influx in Human Sperm. Given that MPA, a synthetic progestin, and the structurally related 17α-acetoxyprogesterone showed little activity in the assay at concentrations up to 10 μM, a series of clinically used progestins, antiprogestins and androgens (structures in Supplemental Fig. 6) were tested in the calcium influx assay (Table 3). Whereas the synthetic progestin drospirenone (**31**) was moderately active, the two antiprogestins ulipristal and mifepristone (**32** and **33**) were weak activators (Fig. 6). As observed for the PROG analogs, acetylation of the 17α-hydroxy group present in ulipristal to yield ulipristal acetate (**34**) further reduced activity. The progestins LNG (**5**) and segesterone acetate (**35**), which bear C17 modifications of ethynyl and acetoxy groups, respectively, produced little calcium influx (Table 3). The inactivity of MPA, LNG, and segesterone acetate further suggests that modification of the D ring with large substituents is not tolerated.

The endogenous steroid hormones testosterone and 17β-estradiol (**36** and **37**) had moderate potency for eliciting sperm calcium uptake, consistent with previous reports (Blackmore et al., 1990; Brenker et al., 2018b; Rehfeld et al., 2020; Jeschke et al., 2021), but contrasting with another study that found no CatSper activation by these steroids (Mannowetz et al., 2017). Given the activity of testosterone, 11β-methyl-19-nortestosterone (11β-MNT, **38**) and 7α-methyl-19-nortestosterone (7α-MNT, **39**) were tested. These synthetic androgens had similar moderate activity, although they were 2- to 3-fold less potent than their parent androgen, testosterone, and were 120- to 150-fold less potent than PROG. Both 7α,11β-, and 7β,11β-dimethylandrolone (DMA) (**40** and **41**, respectively) were weak activators, following trends that modifications to the B ring reduce potency. Interestingly, 7β,11β-DMA exhibited a maximum effect (E_{max}) of only 42% of PROG, the only low efficacy activator observed among the tested compounds (Fig. 6). 7β,11β-DMA may be a weak partial agonist, although its efficacy could be limited by low solubility. Finally, the endogenous mineralocorticoid ALDO (**6**) did not increase $[Ca^{2+}]_i$ at concentrations up to 10 μM.

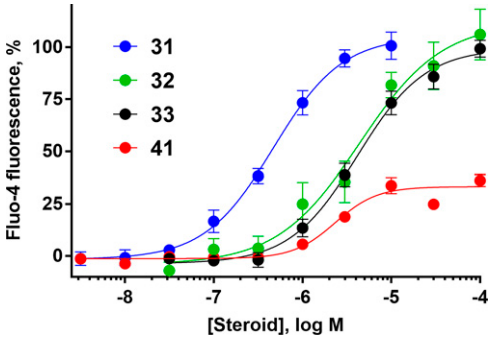

Fig. 6. Several clinically used progestins, antiprogestins, and androgens elicit calcium influx in human sperm. Concentration-response curves for **31**, drospirenone; **32**, ulipristal; **33**, mifepristone; **41**, 7β,11β-dimethylandrolone. Data are plotted as mean ±SEM and expressed as a percent of the response produced by a saturating concentration of PROG (3 μM). EC_{50}, E_{max}, and n values are in Table 3.

Steroidal Inhibitors of Calcium Influx. As MPA, LNG, and ALDO showed negligible activity up to 10 μM, they were tested for their ability to reduce calcium influx produced by PROG, PGE_1, *l*-sirenin, and high K^+/high pH. MPA, LNG, and ALDO produced concentration-dependent decreases in calcium influx elicited by EC_{80} concentrations of PROG, PGE_1, and *l*-sirenin (Fig. 7 and Supplemental Figs. 7–9). MPA was the most potent steroidal inhibitor identified with pIC_{50} values ranging from 5.21 to 5.01 corresponding to IC_{50} values of 6.1 to 9.7 μM for the three activators (Table 4, Fig. 7B–D). LNG and ALDO had similar potency but were weaker inhibitors than MPA (pIC_{50} values ranged from 4.52 to 4.09, corresponding to IC_{50} values of 30 to 82 μM). In contrast, these steroidal inhibitors produced little or no reduction in calcium influx elicited by high K^+/high pH (IC_{50} values > 100 μM; Table 4, Fig. 7E).

T-type CCBs and Steroidal Inhibitors Inhibit Calcium Influx via Different Mechanisms. Three lines of evidence indicate that the steroid inhibitors act by a distinct mechanism from the T-type CCBs. First, mibefradil and ML218 block high K^+/high pH-induced calcium influx, but the steroid inhibitors do not. Second, 30 μM mibefradil reduced the E_{max} for all steroid activators without an appreciable change in their EC_{50} values (Tables 2 and 3). More detailed studies showed that increasing concentrations of mibefradil and ML218 reduced the E_{max} values (Table 5) for PROG (Fig. 8), PGE_1 (Supplemental Fig. 10), and *l*-sirenin (Supplemental Fig. 11) but had little effect on their EC_{50} values, indicating an insurmountable block consistent with noncompetitive inhibition (Fig. 8, Supplemental Figs. 10 and 11). Third, increasing concentrations of MPA, LNG, and ALDO produced rightward parallel shifts of the concentration-response curves for PROG (Fig. 9), PGE_1 (Supplemental Fig. 10), and *l*-sirenin (Supplemental Fig. 11) with little change in their E_{max} values, indicating that the inhibition was completely surmountable with increasing concentrations of the activators, consistent with competitive inhibition. For example, preincubation of sperm with 30 μM MPA caused a 16-fold reduction in the potency of PROG (Table 5). Given this apparent competitive inhibition, both Schild analysis (Fig. 9, Supplemental Figs. 10 and 11) (Arunlakshana and Schild, 1959) and the more generalized Leff-Dougall approach (Leff and Dougall, 1993) were employed to obtain pK_B values, which are the most reliable affinity estimates for competitive antagonists in functional assays (Table 6). The affinity of MPA derived from Leff-Dougall analysis averaged across the activators (PROG, PGE_1, and *l*-sirenin) provided a mean pK_B value 5.78 ± 0.51 (mean ±SD), which corresponds to a K_B value of 1.6 μM. Similarly, Schild analysis provided an average pK_B value of 5.60 ± 0.52 (K_B = 2.5 μM) for MPA. Averaged across the activators, mean ±SD pK_B values for LNG and ALDO were 5.35 ± 0.24 (K_B = 4.5 μM) and 5.29 ± 0.15 (K_B = 5.1 μM), respectively, by Leff-Dougall analysis and 4.80 ± 1.78 (K_B = 16 μM) and 4.44 ± 1.17 (K_B = 36 μM), respectively, by Schild analysis. As expected, neither the

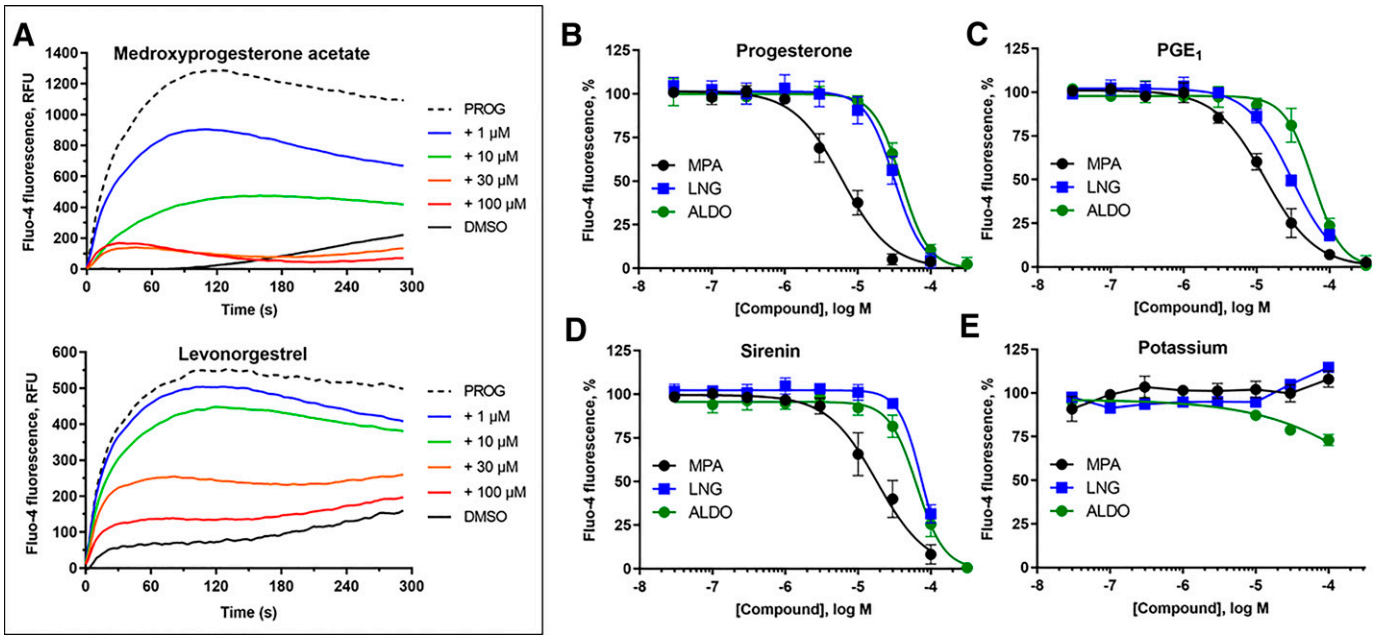

Fig. 7. The steroids MPA, LNG, and ALDO inhibit PROG-, PGE_1-, and *l*-sirenin-induced calcium influx in human sperm. (A) Representative FLIPR traces showing concentration-dependent reduction of PROG-mediated increase in $[Ca^{2+}]_i$ by MPA (upper) and LNG (lower). FLIPR traces for inhibition of PGE_1- and *l*-sirenin-induced calcium influx by MPA and LNG are in Supplemental Figs. 7 and 8, respectively, and traces for ALDO antagonism of all three activators are in Supplemental Fig. 9. (B–E) Potencies of MPA, LNG, or ALDO for inhibiting (B) PROG-, (C) PGE_1-, (D) *l*-sirenin-, or (E) high K^+/high pH-induced calcium influx. Ligand-induced activation used EC_{80} concentrations of activator (30 nM PROG, 10 nM PGE_1, 3 μM *l*-sirenin). Buffer containing 140 mM K^+, pH 8.2 was added to elicit alkalinization/depolarization calcium influx (E). The data in B–E are plotted as the mean ±SEM and expressed as a percent of the response produced by each activator alone. IC_{50} and *n* values are in Table 4.

T-type CCBs nor the steroid antagonists reduced the signal generated by the calcium ionophore A23187 (Supplemental Fig. 12), indicating that none of these compounds act nonspecifically to reduce calcium influx.

Steroidal CatSper Antagonists Selectively Reduce Hyperactivated Motility. The functional effects of CatSper inhibition on sperm motility were evaluated using CASA. Mibefradil inhibited total and progressive motility more potently than ML218 and both completely ablated motility at 30 μM (Fig. 10A). MPA reduced total and progressive motility at 30 μM but not at lower concentrations, whereas LNG and ALDO had no significant effect on total or progressive sperm motility. HAM was evaluated by treating sperm with 100 nM PROG (Fig. 10B) or 100 nM PGE_1 (Supplemental Fig. 13) for 4 hours under capacitating conditions. Mibefradil was more potent than ML218 at inhibiting HAM, and both inhibited HAM more potently than total and progressive motility. Mibefradil and ML218 completely ablated HAM at 10 μM and 30 μM, respectively. Interestingly, the steroidal antagonists had higher selectivity than the T-type CCBs for inhibiting HAM relative to total and progressive motility. Furthermore, even at its highest concentration, MPA did not reduce HAM below the level of the vehicle control, whereas the T-type CCBs ablated all motility at 10 to 30 μM. This observation further indicates differences in the mechanism of action of these classes of compounds.

TABLE 4
Potencies of MPA, LNG, and ALDO to inhibit calcium influx produced by PROG, PGE1, *l*-sirenin, and high K^+/high pH in human sperm

Opener	Antagonist	pIC_{50}	*n*
PROG	MPA	5.18 ± 0.39	12
	LNG	4.49 ± 0.23	9
	ALDO	4.48 ± 0.16	10
PGE_1	MPA	5.01 ± 0.26	11
	LNG	4.52 ± 0.11	6
	ALDO	4.24 ± 0.20	10
l-Sirenin	MPA	5.21 ± 0.33	7
	LNG	4.09 ± 0.05	5
	ALDO	4.21 ± 0.16	9
high K^+/high pH	MPA	<5	4
	LNG	<5	4
	ALDO	<5	4

Inhibitors were evaluated in the presence of an EC_{80} concentration of each activator (30 nM PROG, 10 nM PGE_1, 3 μM *l*-sirenin). Buffer containing 140 mM K^+, pH 8.2 was added to elicit alkalinization/depolarization calcium influx. IC_{50} values are expressed as the mean ±SD with the number of independent experiments indicated by *n*.

Discussion

The most studied tool compounds to explore CatSper physiology and pharmacology are the T-type CCBs mibefradil (Strunker et al., 2011) and NNC55-0396 (Lishko et al., 2011). These and other reported CatSper inhibitors, including HC-056456 (Curci et al., 2021), MDL12330A (Brenker et al., 2012) and RU1968 (Rennhack et al., 2018), also inhibit the sperm-specific K^+ channel Slo3 with similar potencies, although RU1968 appears to be the most selective for CatSper over Slo3 (Rennhack et al., 2018). In addition, the two structurally related T-type CCBs produce an anomalous calcium influx at elevated concentrations (Strunker et al., 2011), are not selective for CatSper over $Ca_v3.1$, $Ca_v3.2$, and $Ca_v3.3$ T-type calcium channels (Martin et al., 2000) and display cytotoxic effects in sperm (Tamburrino et al., 2014), fibroblasts (unpublished observations), and peripheral blood mononuclear cells (Lijnen et al., 1999). Given these issues

TABLE 5
T-type CCBs mibefradil and ML218 reduce the maximal response, whereas MPA, LNG, and ALDO reduce the potency of PROG-, PGE_1-, and *l*-sirenin-induced calcium influx in human sperm

Inhibitor		Progesterone			PGE_1			*l*-Sirenin		
	Conc., μM	pEC_{50}	E_{max}, %	*n*	pEC_{50}	E_{max}, %	*n*	pEC_{50}	E_{max}, %	*n*
MBF	1	8.71 ± 0.29	90	3	8.16 ± 0.08	87	3	5.71 ± 0.01	87	2
	10	8.14 ± 0.20	69	4	8.53 ± 0.37	53	4	5.57 ± 0.41	58	4
	30	8.31 ± 0.42	23	4	8.23 ± 0.51	41	3	5.37 ± 0.51	20	4
	100	8.26 ± 0.24	16	3	—	<10	5	—	<10	3
ML218	1	8.12 ± 0.13	83	3	8.20 ± 0.10	73	3		ND	
	10	7.77 ± 0.35	42	3	8.01 ± 0.05	64	3	5.61 ± 0.45	38	2
	30	—	<10	3	7.86 ± 0.04	15	3	—	4	2
	100	—	<10	3	—	<10	2	—	2	2
MPA	10	7.69 ± 0.40	106	3	7.83 ± 0.43	111	3	5.56 ± 0.15	108	3
	30	7.51 ± 0.38	99	3	7.34 ± 0.15	105	3	5.24 ± 0.58	100[a]	3
	100	6.64 ± 0.07	100[a]	3	6.96 ± 0.03	100[a]	3	4.71 ± 0.21	100[a]	3
LNG	10	7.58 ± 0.16	110	8	7.78 ± 0.30	96	4	5.16 ± 0.08	95	4
	30	7.06 ± 0.26	100[a]	4	7.48 ± 0.18	106	4	4.83 ± 0.16	102	4
	100	6.64 ± 0.06	100[a]	4	7.29 ± 0.22	117	4	4.52 ± 0.03	100[a]	3
ALDO	10	7.44 ± 0.14	114	4	7.88 ± 0.22	107	4	5.28 ± 0.28	104	4
	30	7.09 ± 0.36	106	4	7.82 ± 0.31	99	4	5.10 ± 0.24	109	4
	100	6.59 ± 0.16	100[a]	4	7.44 ± 0.31	100[a]	4	4.51 ± 0.21	100[a]	4

EC_{50} values are expressed as the mean ±SD, and E_{max} values are the percent of a saturating concentration of PROG (3 μM). The number of independent experiments is indicated by *n*. EC_{50}, E_{max}, and *n* values for PROG, PGE_1, and *l*-sirenin in the absence of inhibitor are in Table 2. Fitted parameters were not calculated for conditions producing $E_{max} < 10$.
[a] Constrained value due to rightward shift of dose response.

and their lack of structural diversity, better tool compounds from different structural classes would be helpful to clarify the pharmacology of CatSper. In this study, we show for the first time that the orally active T-type CCB ML218 (Xiang et al., 2011) blocks all modes of evoking calcium influx in sperm, including PROG, PGE_1, *l*-sirenin, and high K^+/high pH, and reduced all types of human sperm motility. With a potency similar to mibefradil and lacking calcium influx at high concentrations, ML218 serves as a useful tool compound to inhibit CatSper. Like the other T-type CCBs, ML218 has higher potency for inhibiting $Ca_v3.1$, $Ca_v3.2$, and $Ca_v3.3$ (Xiang et al., 2011) than CatSper.

A wide variety of small molecules, including steroids (Lishko et al., 2011; Strunker et al., 2011; Mannowetz et al., 2017), the fungal sexual pheromone *l*-sirenin (Syeda et al., 2016), endocrine disrupting chemicals (Brenker et al., 2012; Brenker et al., 2018b) and odorants (Schiffer et al., 2014) activate CatSper. We have explored modifications encompassing the entire steroid skeleton and show that over 30 steroids elicit a CatSper-mediated calcium influx, providing structural insights into the activation of CatSper by steroids (Fig. 11). All modifications reduced potency relative to PROG, generally without affecting the maximal extent of calcium influx. Modifications of the A ring (**10–18**) greatly reduced potency relative to PROG consistent with the activation of CatSper by a C3-linked BSA–PROG conjugate (Lishko et al., 2011). Small substitutions of the B and C rings produced moderately active CatSper activators (**19–24**). Sterically demanding substituents in the C ring (**32–34**) greatly reduced potency, consistent with the inactivity of a C11-linked BSA-PROG conjugate (Lishko et al., 2011). The weak CatSper activation potency of the PROG antagonist mifepristone and its inability to block the PROG-induced activation of CatSper (Lishko et al., 2011; Strunker et al., 2011) serves as an example of the difference in the pharmacology of CatSper and the PROG nuclear hormone receptor. Bulky modifications of the D-ring of the scaffold produce a much greater diminution of activity, suggesting that this portion of the

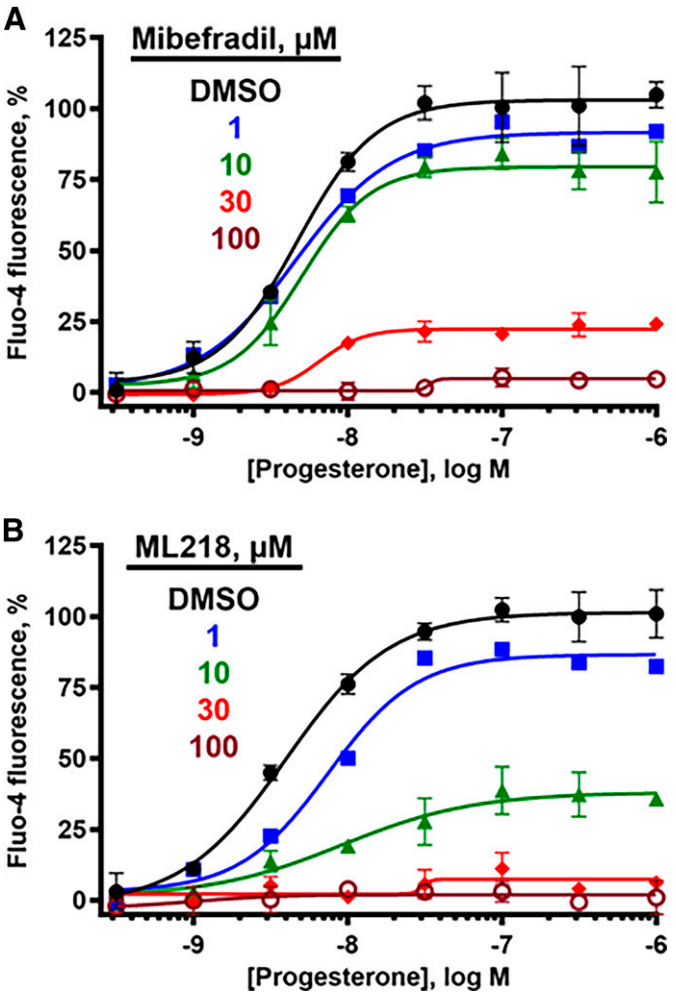

Fig. 8. T-type CCBs produce an insurmountable block of PROG-induced calcium influx in human sperm. (A) Mibefradil and (B) ML218 reduce the PROG E_{max} in a concentration-dependent manner with little change in EC_{50} values, indicating an insurmountable inhibition. E_{max}, EC_{50}, slopes, and *n* values are in Table 5. The data are plotted as the mean ±SEM and expressed as a percent of the response produced by a saturating concentration of PROG (3 μM).

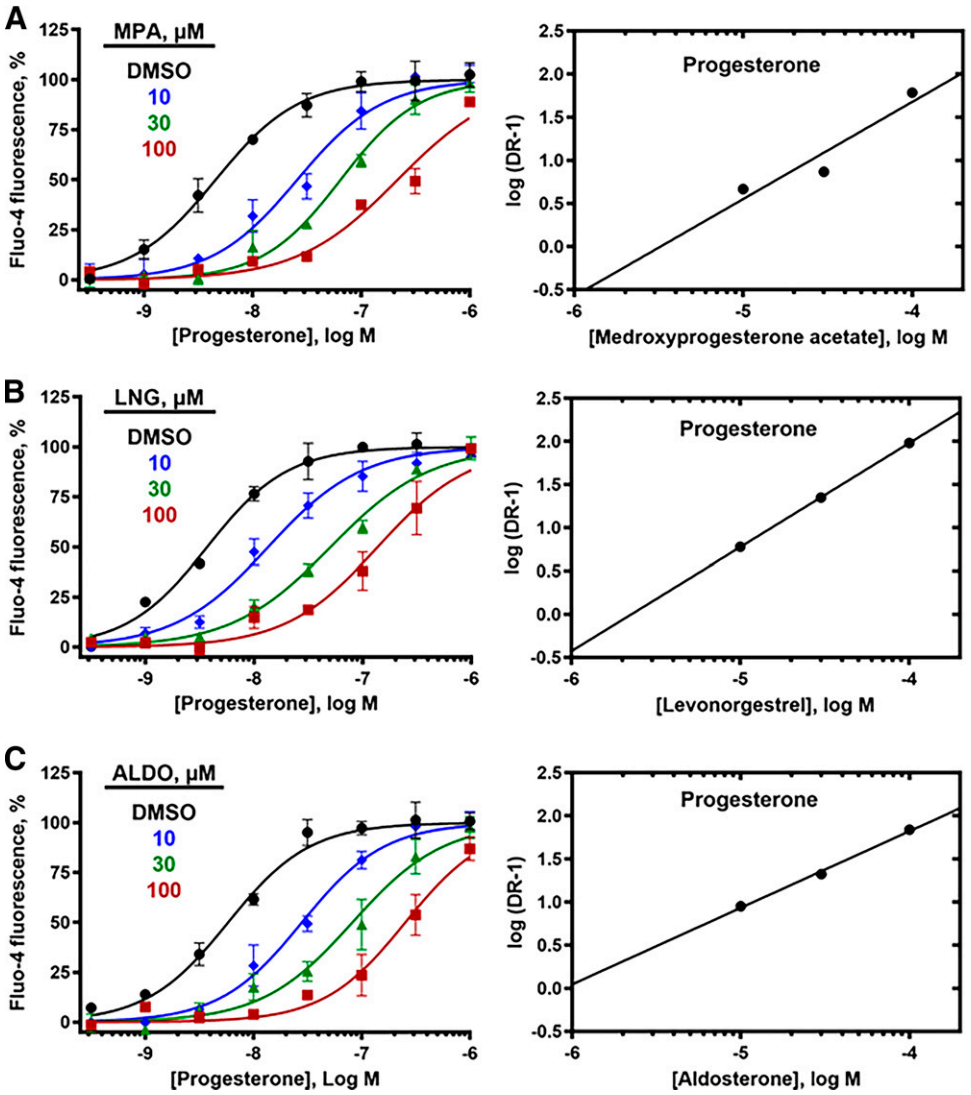

Fig. 9. MPA, LNG, and ALDO produce a surmountable inhibition of PROG-induced calcium influx in human sperm. Increasing concentrations of (A) MPA, (B) LNG, and (C) ALDO increase the observed EC_{50} values for PROG with little change in E_{max} values (left panels). The same data are plotted in the Schild analyses (right panels) indicating surmountable inhibition. E_{max}, EC_{50}, and n values are in Table 5, and pK_B values are in Table 6. The data are plotted as the mean ±SEM and expressed as a percent of the response produced by a saturating concentration of PROG (3 μM).

steroid plays an important role in CatSper activation. Whereas 17α-hydroxylation (**25**) reduced activity slightly consistent with previous reports (Blackmore et al., 1990; Jeschke et al., 2021), calcium influx is largely or completely ablated for compounds with other modifications at the C17 position (**4**, **29**, **34, 35**), particularly when combined with changes at the C18 position (**5, 6**), and for the C20 ketalized steroids. The observed steroid SAR, including the low activity of steroids with modified D rings, is consistent with previous studies of steroid-induced calcium influx (Blackmore et al., 1990; Jeschke et al., 2021). Interestingly, several steroid activators were shown to activate CatSper by binding to the same site (Jeschke et al., 2021).

TABLE 6

Dissociation constants for steroidal antagonists of activator-induced calcium influx in human sperm

Opener	Antagonist	Schild	Leff-Dougall
		pK_B	
PROG	MPA	6.19 ± 1.75	6.16 ± 0.39
	LNG	6.80 ± 0.10	5.47 ± 0.23
	ALDO	5.38 ± 0.27	5.46 ± 0.16
PGE_1	MPA	5.38 ± 0.59	6.00 ± 0.26
	LNG	3.36 ± 0.41	5.50 ± 0.11
	ALDO	3.14 ± 0.95	5.22 ± 0.20
l-Sirenin	MPA	5.22 ± 0.33	5.20 ± 0.20
	LNG	4.25 ± 0.23	5.07 ± 0.05
	ALDO	4.82 ± 1.03	5.19 ± 0.16

The Schild pK_B values (mean ± standard error) were obtained using the EC_{50} values corresponding to the pEC_{50} values listed in Table 5 derived from 3–8 independent experiments. For all Schild analyses, the slopes of the regression lines had values of 1.0 within the 95% CI. The Leff-Dougall pK_B values (mean ± SD) were obtained using the IC_{50} values corresponding to the pIC_{50} values listed in Table 4 derived from 5–12 independent experiments.

Mibefradil blocked the calcium influx produced by every steroid, indicating that their activity is due to CatSper activation. Moreover, both mibefradil and ML218 produced an insurmountable inhibition of the calcium influx produced by PROG, PGE_1, and *l*-sirenin, indicating that these T-type CCBs inhibit CatSper at a site distinct from that of these openers. The T-type CCBs likely block the CatSper pore, since mibefradil blocks sodium channels by binding to the inner pore region of the channels at or near a conserved Asn residue (McNulty et al., 2006), consistent with blockade of both ligand- and depolarization/alkalinization-induced CatSper activation.

MPA, LNG, and ALDO inhibit PROG-, PGE_1-, and *l*-sirenin-induced calcium influx but have no effect on activation

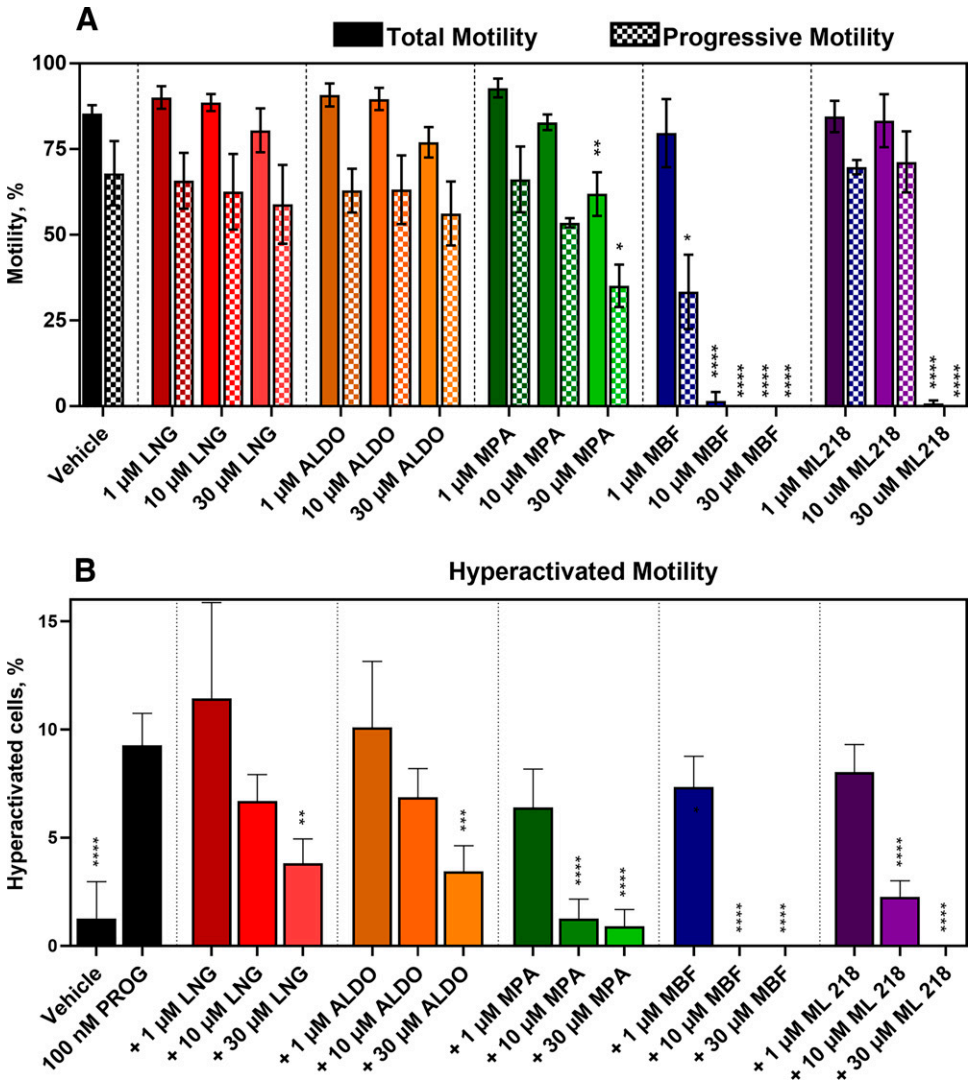

Fig. 10. T-type CCBs inhibit total, progressive, and hyperactivated motility, whereas steroidal CatSper antagonists selectivity inhibit hyperactivated motility in human sperm. **A.** Total (solid) and progressive (checkered) motility was monitored by CASA in the presence of increasing concentrations of inhibitor. The steroidal antagonists LNG, ALDO, and MPA show little or no effect on total and progressive motility, whereas MBF and ML218 completely block these motility parameters. Asterisks indicate differences from vehicle control. **B.** HAM was induced with 100 nM PROG under capacitating conditions. The steroidal CatSper antagonist MPA reduced the percentage of sperm cells displaying HAM to the level of the vehicle control, whereas LNG and ALDO were less potent. The T-type CCBs MBF and ML218 reduced the percentage of sperm cells displaying HAM to zero. Asterisks indicate differences from the PROG only control. In both **A** and **B**, data are presented as mean ±SD and are expressed as a percent of the total sperm cell population analyzed. Statistical significance: * $p < 0.05$, ** $p < 0.005$ and **** $p < 0.0001$.

by high K^+/high pH, suggesting that they prevent the binding of small molecule activators rather than blocking all modes of channel activation like the T-type CCBs. Moreover, the steroid inhibitors MPA, LNG, and ALDO produced a surmountable inhibition of PROG, PGE_1, and *l*-sirenin, consistent with competitive antagonism of each opener by each antagonist, with MPA being the most potent antagonist identified (mean K_B = 1.6 μM, Leff-Dougall analysis). The competitive antagonism of PROG by MPA, LNG, and ALDO indicates that specific structural modifications of the steroid scaffold convert CatSper activators into antagonists, acting at a shared binding site. Indeed, these steroid antagonists all contain D-ring modifications, suggesting that alteration of this region of the steroid scaffold should be the focus of synthetic efforts to identify more potent steroidal CatSper antagonists.

PROG activates α/β hydrolase domain-containing protein 2 (ABHD2), which cleaves 2-arachidonoylglycerol (2AG), depletes it from the membrane, and removes its tonic block of CatSper, facilitating activation of CatSper and subsequent calcium influx (Miller et al., 2016). MPA, LNG, and ALDO may competitively displace PROG from its regulatory site on ABHD2. These steroid antagonists also inhibit the structurally unrelated PGE_1 and *l*-sirenin in a surmountable manner, suggesting competitive antagonism and implying that the binding sites for these activators are the same or overlap with PROG. However, previous studies concluded that PGE_1 and PROG bind distinct sites based on lack of crossdesensitization, additivity at saturating concentrations, and synergism (Schaefer et al., 1998; Brenker et al., 2018a; Lishko et al., 2011; Strunker et al., 2011). Inhibition of ABHD2 by the serine hydrolase inhibitor methoxy arachidonyl fluorophosphonate (MAFP) had no effect on PGE_1-stimulated CatSper currents, suggesting that PGE_1 binds directly to CatSper, possibly by competing with 2AG for its site or at a unique PGE_1 activator site (Miller et al., 2016). Therefore, MPA, LNG, and ALDO may bind to both the PGE_1 and 2AG sites with similar affinity or to a single site for PGE_1 and 2AG on CatSper.

The 4-azasteroid 5α-reductase inhibitor finasteride inhibited PGE_1- but not PROG-induced calcium signals in human sperm, and competition studies suggest that finasteride may be an antagonist of the PGE_1 binding site (Birch et al., 2021). Although its mechanism is complex, finasteride inhibition of

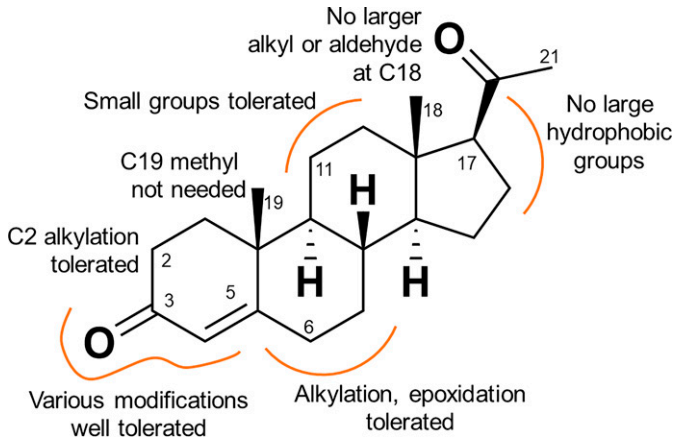

Fig. 11. SAR of CatSper activation by progesterone analogs.

PGE_1-induced calcium influx corroborates our findings that steroids may compete with the structurally unrelated prostaglandin. Surprisingly, the closely structurally related azasteroid 5α-reductase inhibitor dutasteride produced a mixed-type inhibition of PROG- but not PGE_1-induced activation of CatSper (Birch et al., 2021). Antagonism of PROG- and PGE_1-induced activation of CatSper by the 17 substituted steroids dutasteride and finasteride, respectively, strengthens our hypothesis that substitution of the steroid D ring can produce antagonists of ligand-induced CatSper activation. The steroidal sigma receptor ligand RU1968 inhibits human CatSper activation by PROG and PGE_1 (IC_{50} = 5.7 μM) and also inhibits alkalization/depolarization-induced CatSper activation in both mouse and human sperm (IC_{50} 0.83 and 1.2 μM, respectively), suggesting that it binds residues in the pore region and blocks ion flux in a manner similar to the T-type CCBs (Rennhack et al., 2018). Our results indicate that MPA, LNG, and ALDO are not channel pore blockers and may be the first known pure competitive antagonists of PROG-induced CatSper activation.

The different mechanisms of action of mibefradil as a channel pore blocker and MPA, LNG, and ALDO as PROG antagonists implies that they should have different profiles for disruption of CatSper-mediated sperm function. MPA completely inhibited HAM elicited by both PROG and PGE_1 and was more potent than either LNG or ALDO, consistent with the higher potency of MPA for antagonizing PROG- and PGE_1-induced calcium influx. Moreover, the steroid antagonists had higher selectivity than mibefradil and ML218 for inhibiting HAM relative to total and progressive motility. In addition, MPA reduced HAM to the no activator control level, whereas mibefradil and ML218 completely ablated HAM as well as total and progressive motility, possibly by inhibiting ion channels other than CatSper. Since CatSper is required for HAM, the selective inhibition of HAM by MPA, LNG, and ALDO is entirely consistent with their inhibition of CatSper activation. Therefore, these steroid inhibitors are useful tool compounds to more selectivity block activator-induced CatSper-mediated calcium influx and CatSper-dependent sperm function. Regarding potential clinical implications, the concentrations required for complete inhibition of CatSper and HAM are well above those found in human plasma for ALDO (Nowaczynski et al., 1967) and the synthetic progestins, even when the latter are taken at a high dose for emergency contraception (Humpel et al., 1978; Salimtschik et al., 1980). However, it is tempting to speculate that the suppression of sperm motility produced by high dose MPA combined with testosterone in men (Faundes et al., 1981; Wu and Aitken, 1989) may result in concentrations of MPA in the testes that partially inhibit CatSper function and contribute to lower sperm motility. MPA inhibits CatSper with a potency similar to mibefradil but has higher selectivity for inhibiting CatSper-mediated motility, suggesting that MPA is a superior starting point to discover potent, selective antagonists of progesterone-induced CatSper activation as male contraceptive agents.

In summary, we have identified MPA, LNG, and ALDO as competitive antagonists of PROG- and PGE_1-induced CatSper activation and selective inhibitors of HAM in human sperm. Their activity contrasts with the channel pore blockers mibefradil and ML218, which profoundly inhibit all types of motility. These steroidal CatSper antagonists may be more selective than other tool compounds to study CatSper-mediated sperm function.

Acknowledgments

The authors would like thank Dr. Rawle Francis for developing and validating the FLIPR assay and helpful discussions, Dr. Subhashree Francis for purity analysis of purchased steroids and control compounds, Dr. Henry Wong for serving as primary donor recruiter and liaison, and the donors involved in the project. A special and sincere thank you to Drs. Min Lee and Diana Blithe from NICHD for their discussions and support of this project, including the gifting of several synthetic androgens.

Authorship Contributions

Participated in research design: Carlson, Georg, Hawkinson.
Conducted experiments: Carlson.
Performed data analysis: Carlson, Georg, Hawkinson.
Wrote or contributed to the writing of the manuscript: Carlson, Georg, Hawkinson.

References

Arunlakshana O and Schild HO (1959) Some quantitative uses of drug antagonists. *Br J Pharmacol Chemother* **14**:48–58.
Avenarius MR, Hildebrand MS, Zhang Y, Meyer NC, Smith LL, Kahrizi K, Najmabadi H, and Smith RJ (2009) Human male infertility caused by mutations in the CATSPER1 channel protein. *Am J Hum Genet* **84**:505–510.
Avidan N, Tamary H, Dgany O, Cattan D, Pariente A, Thulliez M, Borot N, Moati L, Barthelme A, Shalmon L, et al. (2003) CATSPER2, a human autosomal nonsyndromic male infertility gene. *Eur J Hum Genet* **11**:497–502.
Birch MR, Dissing S, Skakkebæk NE, and Rehfeld A (2021) Finasteride interferes with prostaglandin-induced CatSper signalling in human sperm. *Reproduction* **161**:561–572.
Blackmore PF, Beebe SJ, Danforth DR, and Alexander N (1990) Progesterone and 17 alpha-hydroxyprogesterone. Novel stimulators of calcium influx in human sperm. *J Biol Chem* **265**:1376–1380.
Brenker C, Goodwin N, Weyand I, Kashikar ND, Naruse M, Krähling M, Müller A, Kaupp UB, and Strünker T (2012) The CatSper channel: a polymodal chemosensor in human sperm. *EMBO J* **31**:1654–1665.
Brenker C, Rehfeld A, Schiffer C, Kierzek M, Kaupp UB, Skakkebæk NE, and Strünker T (2018a) Synergistic activation of CatSper Ca2+ channels in human sperm by oviductal ligands and endocrine disrupting chemicals. *Hum Reprod* **33**:1915–1923.
Brenker C, Schiffer C, Wagner IV, Tüttelmann F, Röpke A, Rennhack A, Kaupp UB, and Strünker T (2018b) Action of steroids and plant triterpenoids on CatSper Ca^{2+} channels in human sperm. *Proc Natl Acad Sci USA* **115**:E344–E346.
Brown SG, Miller MR, Lishko PV, Lester DH, Publicover SJ, Barratt CLR, and Martins Da Silva S (2018) Homozygous in-frame deletion in CATSPERE in a man producing spermatozoa with loss of CatSper function and compromised fertilizing capacity. *Hum Reprod* **33**:1812–1816.
Chung JJ, Miki K, Kim D, Shim SH, Shi HF, Hwang JY, Cai X, Iseri Y, Zhuang X, and Clapham DE (2017) CatSperζ regulates the structural continuity of sperm Ca^{2+} signaling domains and is required for normal fertility. *eLife* **6**:e23082.

Chung JJ, Navarro B, Krapivinsky G, Krapivinsky L, and Clapham DE (2011) A novel gene required for male fertility and functional CATSPER channel formation in spermatozoa. *Nat Commun* **2**:153.
Curci L, Carvajal G, Sulzyk V, Gonzalez SN, and Cuasnicú PS (2021) Pharmacological inactivation of CatSper blocks sperm fertilizing ability independently of the capacitation status of the cells: implications for non-hormonal contraception. *Front Cell Dev Biol* **9**:686461.
Dosa PI and Amin EA (2016) Tactical approaches to interconverting GPCR agonists and antagonists. *J Med Chem* **59**:810–840.
Faúndes A, Brache V, León P, Schmidt F, and Alvarez-Sánchez F (1981) Sperm suppression with monthly injections of medroxyprogesterone acetate combined with testosterone enanthate at a high dose (500 mg). *Int J Androl* **4**:235–245.
Hildebrand MS, Avenarius MR, Fellous M, Zhang Y, Meyer NC, Auer J, Serres C, Kahrizi K, Najmabadi H, Beckmann JS et al. (2010) Genetic male infertility and mutation of CATSPER ion channels. *Eur J Hum Genet* **18**:1178–1184.
Hümpel M, Wendt H, Pommerenke G, Weiss C, and Speck U (1978) Investigations of pharmacokinetics of levonorgestrel to specific consideration of a possible first-pass effect in women. *Contraception* **17**:207–220.
Hwang JY, Mannowetz N, Zhang Y, Everley RA, Gygi SP, Bewersdorf J, Lishko PV, and Chung JJ (2019) Dual sensing of physiologic pH and calcium by EFCAB9 regulates sperm motility. *Cell* **177**:1480–1494.e19.
Jeschke JK, Biagioni C, Schierling T, Wagner IV, Börgel F, Schepmann D, Schüring A, Kulle AE, Holterhus PM, von Wolff M, et al. (2021) The action of reproductive fluids and contained steroids, prostaglandins, and Zn^{2+} on CatSper Ca^{2+} channels in human sperm. *Front Cell Dev Biol* **9**:699554.
Kirichok Y, Navarro B, and Clapham DE (2006) Whole-cell patch-clamp measurements of spermatozoa reveal an alkaline-activated Ca2+ channel. *Nature* **439**:737–740.
Leff P and Dougall IG (1993) Further concerns over Cheng-Prusoff analysis. *Trends Pharmacol Sci* **14**:110–112.
Lijnen P, Fagard R, and Petrov V (1999) Mibefradil-induced inhibition of proliferation of human peripheral blood mononuclear cells. *J Cardiovasc Pharmacol* **33**:595–604.
Lin S, Ke M, Zhang Y, Yan Z, and Wu J (2021) Structure of a mammalian sperm cation channel complex. *Nature* **595**:746–750.
Lishko PV, Botchkina IL, and Kirichok Y (2011) Progesterone activates the principal Ca2+ channel of human sperm. *Nature* **471**:387–391.
Liu J, Xia J, Cho KH, Clapham DE, and Ren D (2007) CatSperbeta, a novel transmembrane protein in the CatSper channel complex. *J Biol Chem* **282**:18945–18952.
Luo T, Chen HY, Zou QX, Wang T, Cheng YM, Wang HF, Wang F, Jin ZL, Chen Y, Weng SQ, et al. (2019) A novel copy number variation in CATSPER2 causes idiopathic male infertility with normal semen parameters. *Hum Reprod* **34**:414–423.
Luo T, Wang F, Weng S, Chen H, Kang H, Wang J, and Luo S (2020) Anethole compromises human sperm function by affecting the sperm intracellular calcium concentration and tyrosine phosphorylation. *Reprod Toxicol* **93**:99–105.
Mannowetz N, Miller MR, and Lishko PV (2017) Regulation of the sperm calcium channel CatSper by endogenous steroids and plant triterpenoids. *Proc Natl Acad Sci USA* **114**:5743–5748.
Martin RL, Lee JH, Cribbs LL, Perez-Reyes E, and Hanck DA (2000) Mibefradil block of cloned T-type calcium channels. *J Pharmacol Exp Ther* **295**:302–308.
McNulty MM, Kyle JW, Lipkind GM, and Hanck DA (2006) An inner pore residue (Asn406) in the Nav1.5 channel controls slow inactivation and enhances mibefradil block to T-type Ca2+ channel levels. *Mol Pharmacol* **70**:1514–1523.
Miller MR, Mannowetz N, Iavarone AT, Safavi R, Gracheva EO, Smith JF, Hill RZ, Bautista DM, Kirichok Y, and Lishko PV (2016) Unconventional endocannabinoid signaling governs sperm activation via the sex hormone progesterone. *Science* **352**:555–559.
Morris J, Jones S, Howl J, Lukanowska M, Lefievre L, and Publicover S (2015) Cell-penetrating peptides, targeting the regulation of store-operated channels, slow decay of the progesterone-induced [Ca2+]i signal in human sperm. *Mol Hum Reprod* **21**:563–570.
Nowaczynski W, Silah J, and Genest J (1967) Procedure for determination of aldosterone in human peripheral plasma by double-isotope derivative assay, and its application for measurement of secretory rate and urinary excretion. *Can J Biochem* **45**:1919—1936.
Qi H, Moran MM, Navarro B, Chong JA, Krapivinsky G, Krapivinsky L, Kirichok Y, Ramsey IS, Quill TA, and Clapham DE (2007) All four CatSper ion channel proteins are required for male fertility and sperm cell hyperactivated motility. *Proc Natl Acad Sci USA* **104**:1219–1223.
Quill TA, Ren D, Clapham DE, and Garbers DL (2001) A voltage-gated ion channel expressed specifically in spermatozoa. *Proc Natl Acad Sci USA* **98**:12527–12531.
Quill TA, Sugden SA, Rossi KL, Doolittle LK, Hammer RE, and Garbers DL (2003) Hyperactivated sperm motility driven by CatSper2 is required for fertilization. *Proc Natl Acad Sci USA* **100**:14869–14874.
Rehfeld A, Andersson AM, and Skakkebæk NE (2020) Bisphenol A diglycidyl ether (BADGE) and bisphenol analogs, but not bisphenol A (BPA), activate the CatSper Ca^{2+} channel in human sperm. *Front Endocrinol (Lausanne)* **11**:324.
Ren D, Navarro B, Perez G, Jackson AC, Hsu S, Shi Q, Tilly JL, and Clapham DE (2001) A sperm ion channel required for sperm motility and male fertility. *Nature* **413**:603–609.
Rennhack A, Schiffer C, Brenker C, Fridman D, Nitao ET, Cheng YM, Tamburrino L, Balbach M, Stölting G, Berger TK, et al. (2018) A novel cross-species inhibitor to study the function of CatSper Ca^{2+} channels in sperm. *Br J Pharmacol* **175**:3144–3161.
Salimtschik M, Mouridsen HT, Loeber J, and Johansson E (1980) Comparative pharmacokinetics of medroxyprogesterone acetate administered by oral and intramuscular routes. *Cancer Chemother Pharmacol* **4**:267–269.
Schaefer M, Hofmann T, Schultz G, and Gudermann T (1998) A new prostaglandin E receptor mediates calcium influx and acrosome reaction in human spermatozoa. *Proc Natl Acad Sci USA* **95**:3008–3013.
Schiffer C, Müller A, Egeberg DL, Alvarez L, Brenker C, Rehfeld A, Frederiksen H, Wäschle B, Kaupp UB, Balbach M, et al. (2014) Direct action of endocrine disrupting chemicals on human sperm. *EMBO Rep* **15**:758–765.
Shimizu Y, Yorimitsu A, Maruyama Y, Kubota T, Aso T, and Bronson RA (1998) Prostaglandins induce calcium influx in human spermatozoa. *Mol Hum Reprod* **4**:555–561.
Shu F, Zhou X, Li F, Lu D, Lei B, Li Q, Yang Y, Yang X, Shi R, and Mao X (2015) Analysis of the correlation of CATSPER single nucleotide polymorphisms (SNPs) with idiopathic asthenospermia. *J Assist Reprod Genet* **32**:1643–1649.
Smith JF, Syritsyna O, Fellous M, Serres C, Mannowetz N, Kirichok Y, and Lishko PV (2013) Disruption of the principal, progesterone-activated sperm Ca2+ channel in a CatSper2-deficient infertile patient. *Proc Natl Acad Sci USA* **110**:6823–6828.
Strünker T, Goodwin N, Brenker C, Kashikar ND, Weyand I, Seifert R, and Kaupp UB (2011) The CatSper channel mediates progesterone-induced Ca2+ influx in human sperm. *Nature* **471**:382–386.
Sun XH, Zhu YY, Wang L, Liu HL, Ling Y, Li ZL, and Sun LB (2017) The Catsper channel and its roles in male fertility: a systematic review. *Reprod Biol Endocrinol* **15**:65.
Syeda SS, Carlson EJ, Miller MR, Francis R, Clapham DE, Lishko PV, Hawkinson JE, Hook D, and Georg GI (2016) The fungal sexual pheromone sirenin activates the human catsper channel complex. *ACS Chem Biol* **11**:452–459.
Tamburrino L, Marchiani S, Minetti F, Forti G, Muratori M, and Baldi E (2014) The CatSper calcium channel in human sperm: relation with motility and involvement in progesterone-induced acrosome reaction. *Hum Reprod* **29**:418–428.
Torrezan-Nitao E, Brown SG, Mata-Martínez E, Treviño CL, Barratt C, and Publicover S (2021) [Ca2+]i oscillations in human sperm are triggered in the flagellum by membrane potential-sensitive activity of CatSper. *Hum Reprod* **36**:293–304.
Wang H, Liu J, Cho KH, and Ren D (2009) A novel, single, transmembrane protein CATSPERG is associated with CATSPER1 channel protein. *Biol Reprod* **81**:539–544.
Wu FC and Aitken RJ (1989) Suppression of sperm function by depot medroxyprogesterone acetate and testosterone enanthate in steroid male contraception. *Fertil Steril* **51**:691–698.
Xiang Z, Thompson AD, Brogan JT, Schulte ML, Melancon BJ, Mi D, Lewis LM, Zou B, Yang L, Morrison R, et al. (2011) The discovery and characterization of ML218: a novel, centrally active t-type calcium channel inhibitor with robust effects in STN neurons and in a rodent model of parkinson's disease. *ACS Chem Neurosci* **2**:730–742.
Yuan Y, Ding X, Cheng Y, Kang H, Luo T, Zhang X, Kuang H, Chen Y, Zeng X, and Zhang D (2020) PFOA evokes extracellular Ca^{2+} influx and compromises progesterone-induced response in human sperm. *Chemosphere* **241**:125074.
Zhang X, Kang H, Peng L, Song D, Jiang X, Li Y, Chen H, and Zeng X (2020) Pentachlorophenol inhibits CatSper function to compromise progesterone's action on human sperm. *Chemosphere* **259**:127493.

Address correspondence to: Jon E. Hawkinson, Institute for Therapeutics Discovery and Development, University of Minnesota, 717 Delaware Street SE, Room 484, Minneapolis, MN 55414. E-mail: hawkinso@umn.edu; or Gunda I. Georg, Institute for Therapeutics Discovery and Development, Department of Medicinal Chemistry, College of Pharmacy, University of Minnesota, 717 Delaware Street SE, Room 452, Minneapolis, MN 55414. E-mail: georg@umn.edu